Spectrum of output noise in diffusion and phonon cooled hot electron superconducting mixers

R.J. Schoelkopf, P.J. Burke, and D.E. Prober
Departments of Applied Physics and Physics, Yale University, 15 Prospect St., New Haven, CT 06520-8284
A.Skalare, W.R. McGrath, B.Bumble, and H.G. LeDuc
Center for Space Microelectronics Technology, Jet Propulsion Laboratory, California Institute of Technology, Pasadena, CA 91109

March 25, 1996

Abstract

Measurements of the spectrum of the output noise of Nb hot-electron mixers are presented. The device lengths vary from 0.08 μm to 3 μm, allowing the investigation of the crossover from phonon to diffusion cooling. The data span the IF range from 75 MHz to 7.5 GHz. The dominant contribution to the noise is thermal fluctuation noise, which is expected to display a one pole rolloff. We present data with 20 GHz LO applied in two cases: with LO power optimized for gain, and LO power optimized for mixer noise. We find that in the optimum gain case, the spectrum is in agreement with simple theoretical predictions, while in the minimum mixer noise case, the output noise is too low ($< 15\ K$) to allow accurate measurements of the spectrum.

1 Introduction

Superconducting hot-electron bolometers are very promising for use in THz receivers. Since the mixing process in these devices is thermal, they are expected to perform well even at frequencies above the energy gap of the superconductor used. For a device to be suitable for use in a heterodyne receiver, it should have both good conversion efficiency and low noise. While many sources of noise can be present, the dominant sources, as with many bolometers, are expected to be Johnson noise and thermal (or energy) fluctuation noise. The fluctuation noise (sometimes also called phonon noise) arises from the thermodynamic fluctuations in the temperature (or energy) of a thermal mass which is connected to a bath via a thermal link. In a superconducting bolometer, these fluctuations in temperature give rise to resistance fluctuations, which in turn lead to voltage fluctuations, due to the bias current.

The maximum rate at which the temperature of the thermal mass (in this case, the temperature of the electrons in the superconductor) can change is limited by the thermal time constant, $\tau_{th} = C/G$. For a bolometric mixer, this can limit the usable IF bandwidth, since the conversion efficiency as a function of IF is given by

$$\frac{\eta(f)}{\eta(0)} = \frac{1}{1+(f/f_{3dB})^2}, \tag{1}$$

where the 3 dB bandwidth is given by $f_{3dB} = 1/2\pi\tau_{th}$[1]. The contribution of thermal fluctuations to the bolometer output noise is expected [2, 3] to the follow the same frequency dependence as Eq. (1). Therefore, the mixer noise temperature ($T_{mix}(DSB) \equiv T_{out}/2\eta$) is predicted to be independent of IF until the thermal fluctuation noise has fallen to the Johnson noise value, at which point the mixer noise will increase rapidly with increasing IF.

The achievable IF bandwidth is an important issue, since typical applications such as remote sensing of atmospheric chemistry and radioastronomy require an IF bandwidth of several GHz. Superconducting hot-electron bolometers using micron-size bridges of Nb rely on the electron-phonon interaction as the cooling mechanism. These have demonstrated an IF bandwidth of $\sim$ 100 MHz[4]. One approach for increasing the IF bandwidth is to use a material with a shorter electron-phonon time such as NbN[5]. Outdiffusion of hot electrons [6] can also lead to increase in IF bandwidth, if the device length, L, is less than $\sqrt{12}\ L_{e-ph}$ (with $L_{e-ph} \equiv \sqrt{D\tau_{e-ph}}$, D the diffusion constant and τ_{e-ph} the inelastic electron-phonon time)[7]. Recently [8], we have demonstrated the crossover from phonon to diffusion cooling in Nb microbridges by measuring the dependence of the 3dB rolloff of the conversion efficiency on length. There, we confirmed the expected L^2 dependence, and demonstrated a bandwidth of over 6 GHz for a 0.08 μm bridge. Previously [9], we demonstrated low noise ($T_{receiver}$=650K, DSB) and a 1.7 GHz IF bandwidth at an LO frequency of 530 GHz, which is above the gap frequency of the 0.24 μm Nb bridge measured there.

In this article we present measurements on the spectrum of the noise for the devices studied in [8]. (Measurements of the noise spectrum of phonon-cooled NbN devices was recently presented in [10].) The longest bridge ($L = 3\mu m$) is in the phonon-cooling limit, while the shortest device is dominantly diffusion cooled. The experiments were performed at an LO frequency of 20 GHz. Under some conditions the noise does indeed seem to obey the form given in Eq (1), with 3dB frequencies in good agreement with those determined in the mixing measurements. This spectral dependence can be interpreted as a confirmation that thermal fluctuations are the dominant noise source.

2 Experimental technique

2.1 Device fabrication and RF coupling:

The devices studied were all fabricated from the same thin (100 Å) Nb film, deposited on a quartz substrate. The patterned film has a transition temperature of $T_c \approx 5.5$ K, transition width $\Delta T_c \sim 0.5\ K$, and sheet resistance $\approx$ 33 Ω. The length of the bridge was defined by the normal metal (1000 Å thick Au) contacts using direct write e-beam lithography in a self-aligned process[11]. The device parameters are given in Table 1. Each device was mounted at the end of a section of 50 Ω microstrip, using a "flip-chip" configuration to assure a broadband match [12]. The mixer mount was housed in a vacuum can, allowing variable temperature measurements to be made from 2 to 20 K. A cooled directional coupler was used to weakly couple in the RF and LO. The through port was connected to a cooled, low noise ($\approx$ 20 K), broadband amplifier. The cable losses, amplifier gain, and coupler performance were each measured at 2 K. The mixer conversion efficiency as a function of intermediate frequency was thus measured to $\pm$ 2 dB.

2.2 Mixer noise measurements:

In order to measure the mixer noise, we used a coolable 1.25-1.75 GHz isolator in front of the amplifier to reduce impedance mismatch effects. The output of the amplifier stage was sent through a 500 MHz filter centered at 1.5 GHz, and then into a crystal detector. An *in situ* calibration of the amplifier noise was carried out by using the Johnson noise of the device in the normal state between 6 and 20 K to calibrate the IF system. The calibration was confirmed in a separate measurement with a variable temperature termination as the Johnson noise source. The noise temperature of the IF gain stage in this configuration was about 20 K. The mixer noise was calculated by referring the measured output noise to the input using the measured conversion efficiency.

2.3 Fluctuation noise spectrum measurements:

Since sufficiently broadband, coolable isolators are not readily available, we decided to carry out the spectral measurements without an isolator. The noise of the amplifier consists of two noise waves at the input: one directed towards the input port, and one directed away from it [13]. We have not measured the magnitude of the noise wave directed toward the device. In order to reduce the effect of the noise wave reflected off the device, we inserted a 3 dB attenuator between the device and the amplifier. An *in situ* calibration was done with the device in the normal state as the noise source as describe above, but at each frequency this time. The output of the IF amplifier chain (gain $\approx$ 70 dB) was sent into a spectrum analyzer with a resolution bandwidth of 3 MHz. 100 to 1000 traces were averaged, and then the data were smoothed over a 100-200 MHz spacing. Therefore, the frequency resolution of the measurement is about 100 MHz. In between measurements of the spectra, we also used the 1.25-1.75 GHz filter as described above to determine quickly the dependence of the noise on dc bias and LO power.

3 Results and analysis:

3.1 Mixer noise results:

The *coupled* conversion efficiency η and the output noise T_{out} were measured at 2.2 K. We varied the LO power and dc bias to achieve optimum conversion efficiency. In this case, the I-V curve is hysteretic. We also find that for an LO power above some critical value, the I-V curve is non-hysteretic and the conversion efficiency, output noise, and mixer noise are smooth functions of bias voltage. This critical value of P_{LO} is 2-3 dB higher than that needed for optimum gain, but the mixer noise temperature T_m is lower by about 25% for P_{LO} just above the critical value. We plot the I-V curve and the conversion efficiency for the two cases in Fig. 1a. In Fig. 1b, the output noise and calculated mixer noise temperature are shown in the two cases. There is a region at low voltage which is inaccessible to dc bias. The load line was 20 Ω, which does not entirely explain this region. For clarity, we have not drawn lines between the supercurrent branch and the resistive branch. The main conclusion of these measurements is that the output noise and conversion gain change significantly with LO power, but the effects approximately cancel each other, so that the mixer noise temperature is not that sensitive to the LO power.

3.2 Fluctuation noise spectrum results:

The measurements carried out here were with 18-20 GHz LO applied. We used two different LO powers for each measurement. In one case, we used just enough LO power to make the I-V curve non-hysteretic. In the second case, we reduced

the LO power to 3 dB below this critical value. This is approximately the value needed for optimum mixer gain. In the"optimum gain case", we used a dc bias as close as possible to the supercurrent, but on the finite-voltage branch; this is the dc bias where optimum gain and minimum mixer noise occurs for this LO power value. In the overpumped case, we used a dc bias where the output noise (measured in the 1.25-1.75 GHz band) was maximum. This is generally not the exact dc bias where minimum mixer noise or maximum conversion efficiency occurs in the overpumped LO power case, as can be seen in figure 1.

In Fig. 2 a-d, we plot the noise and current *vs.* voltage in the overpumped and optimally pumped case. On each plot we indicate the dc bias used to measure the spectrum of the noise.

The noise *vs.* intermediate frequency is plotted in Fig. 3 a,b. In addition, we plot fits to the functional form of Eq. (1), plus a Johnson noise source at 5.5 K. (We assume the electrons are at $T_e \approx 5.5\,K$.) The results of these fits for the two different cases are shown in Table I. In the overpumped case for devices A and B, the noise is very low, and it is difficult to determine the change in noise with change in frequency, since the noise is comparable to the uncertainties in the measurements. If we normalize the spectrum of the noise by its low frequency value, we can compare the spectrum from different devices more clearly. In Fig. 4, the relative magnitude of the thermal fluctuation contribution to the output noise *vs.* frequency is evident. One sees that the spectrum of the phonon cooled device A falls sooner, and that the shortest device has a rolloff of about 6.1 GHz. The inferred thermal time constants are in fairly good agreement with recent results based on mixing measurements on these devices [8].

One possible complication with the interpretation of the measurements comes from the fact that the device impedance is expected to change with frequency, causing a different contribution of the reflected amplifier noise wave at different frequencies. The noise calibration was done with the device in the normal state, where it is very well-matched to the 50 Ohm amplifier input impedance. In this case, the noise wave reflected back towards the amplifier is very small. We also measured the output power of the device in the supercurrent branch, where the reflection coefficient off the device is 1. (In the supercurrent state, R=0, so $\Gamma = 1$.) The output noise inferred in this case was between 10 K and -10 K. Therefore, in the worst case, the error in the measurement due to the imperfect input match at the device (i.e. due to the the reflected noise wave) is $\pm$ 10 K. We believe that the error is actually smaller than this. The device impedance as a function of frequency is expected to relate to the I-V characteristic [14]. In particular, at low frequencies, the device impedance is simply the differential impedance from the I-V curve, while at high frequencies ($f \gg f_{3dB}$), the device impedance is V_{dc}/I_{dc}. We show in Table I the low frequency differential resistance from the I-V curve, as well as V_{dc}/I_{dc}, for the bias points used to measure the spectrum of the noise. In almost all cases, the device is predicted to be fairly well matched to the 50 Ω system. Therefore, the noise wave reflected off the device should be much smaller than what is reflected off the supercurrent.

Thus, the measurement error is probably less than the ± 10 K derived above.

4 Discussion

The spectral dependence of the output noise is in good agreement with the form expected for thermal fluctuations, with thermal time constants which are consistent with those determined via conversion efficiency measurements. This implies that the main contribution to the noise is indeed fluctuation noise. A detailed understanding of the overall scale of this fluctuation noise, however, will be harder to obtain. For example, as is clear from Figs. 1 and 2, the output noise depends on bias voltage very sensitively in the optimum gain case. Therefore, it is difficult to compare the magnitude of the low frequency noise of the four devices in the optimum gain case. In the overpumped case, the noise is not sensitive to the precise bias voltage used, so the comparisons are more reliable. We do not understand at this point why the output noise of the diffusion cooled devices is very low for all frequencies measured, whereas the noise for the phonon-cooled devices is much higher, in the overpumped case. Future experiments will require the simultaneous measurements of output noise and conversion efficiency vs. frequency *and* dc bias. In addition, the LO frequency used here is below the gap frequency for the bridges measured. The LO at this frequency may have a different effect on the output noise than LO's at frequencies above the gap. Nevertheless, the output noise for the diffusion-cooled devices, in the case of optimum gain, is within a factor of two of the output noise measured previously [9] with an LO of 530 GHz, which is well above the gap frequency for $T_C = 5.5$ K. The bandwidths inferred from conversion efficiency measurements at these two LO frequencies were also very similar, further reinforcing the correspondence between the two experiments.

5 Conclusions

We have measured the spectrum of the output noise of diffusion as well as phonon-cooled Nb superconducting mixers. For an applied LO power which optimizes the gain, the spectrum of the noise shows a rolloff in agreement with the measured conversion efficiency rolloff, as expected. For a larger applied LO power, which minimizes the *mixer* noise temperature, we find that the output noise of the phonon-cooled devices obeys a similar behavior to the conversion gain, but the diffusion cooled devices have a very low output noise ($< 15\ K$). While this makes measurements of the output spectrum difficult in this case, it implies that very low noise performance can be obtained in diffusion-cooled devices.

6 Acknowledgements

We thank A.A. Verheijen for contributions to early experiments, and B. Karasik, M. Gaidis, U. Meirav, M. Reznikov, and J. Zmuidzinas for useful discussions. We thank Hewlett Packard for the loan of a network analyzer. The research described in this paper was performed by Yale University and the Center for Space Microelectronics Technology, Jet Propulsion Laboratory, California Institute of Technology, and was jointly sponsored by the NSF and by the NASA Office of Space Access and Technology, and Office of Space Science. Funding for P.J. Burke was provided by a NASA Graduate Student Fellowship as well as a Connecticut High Technology Fellowship.

References

[1] Due to electro-thermal feedback effects (H. Ekström, B. Karasik, E. Kollberg, and K.S. Yngvesson, Proc. of 5th Intl. Symp. on Space THz Tech., U. of Mich., Ann Arbor, MI, 169 (1994)), the time constant inferred from the bandwidth is equal to the "bare" thermal time constant τ_{th} only if the self-heating parameter $[I^2(dR/dT)/G]$ is small or V_{dc}/I_{dc} is close to the IF amplifier input impedance, 50 Ω. (Here G is the thermal conductance to the bath.) Since V_{dc}/I_{dc} is close to 50 Ω for the devices measured in this work, we believe that the inferred time constant is approximately equal to τ_{th}.

[2] L.D. Landau and E.M. Lifshitz, Statistical Physics, Pergamon Press, New York (1980); J.C. Mather, Applied Optics **21**, 1125 (1982).

[3] B.S. Karasik and A.I. Elant'ev, submitted to Appl. Phys. Lett.

[4] E.M. Gershenzon, G.N. Gol'tsman, I.G. Gogidze, Y.P. Gusev, A.I. Elant'ev, B.S. Karasik, and A.D. Semenov, Sov. Phys. Superconductivity **3**, 1582 (1990).

[5] G.N. Gol'tsman, B.S. Karasik, O.V. Okunev, A.L. Dzardanov, E.M. Gershenzon, H. Ekström, S. Jacobsson, and E. Kollberg, IEEE Trans. Appl. Supercond **5**, 3065 (1995).

[6] D.E. Prober, Appl. Phys. Lett., **62**, 2119 (1993).

[7] It is predicted in [6] for cooling by electron diffusion that $\tau_{th} = L^2/(12D)$, where L is the bridge length and D the diffusion constant. Thus, when $L = \sqrt{12}\ L_{e-ph}$, the electron-phonon time τ_{e-ph} is equal to the time constant due to diffusion cooling.

[8] P.J. Burke, R.J. Schoelkopf, D.E. Prober, A. Skalare, W.R. McGrath, B. Bumble, H.G. LeDuc, submitted to Appl. Phys. Lett.

[9] A. Skalare, W.R. McGrath, B. Bumble, H.G. LeDuc, P.J. Burke, A.A. Verheijen, R.J. Schoelkopf, and D.E. Prober, Appl. Phys. Lett., in press, March 11, 1996.

[10] H. Ekström and B. Karasik, Appl. Phys. Lett. **66**, 3212 (1995).

[11] B. Bumble and H.G. LeDuc, unpublished.

[12] The power coupling to the device in the normal state from the cold RF input was measured to be above 90% from 0.1-12 GHz. The match is expected to remain this good to above 20 GHz.

[13] S.A. Maas, Microwave Mixers, Artech House, Boston (1993); P. Penfield, IRE Trans. Circuit Theory **CT-9** 84 (1962).

[14] In the case of phonon-cooled Nb, the impedance has actually been measured (A.I. Elant'ev and B.S. Karasik, Sov. J. Low Temp. Phys. **15** 379 (1990); H. Ekström, B. Karasik, E. Kollberg, and K.S. Yngvesson, Proc. of 5th Intl. Symp on Space THz Technology, University of Michigan, Ann Arbor, MI, 169 (1994)) We assume here the diffusion cooled Nb devices behave in the same way, although this has not yet been measured. The impedance of NbN does not seem to obey the simple frequency dependence that Nb does (H. Ekström, B. Karasik, E. Kollberg, G. Gol'tsman, E. Gershenzon, Proc. of 6th Intl. Symp on Space THz Technology, California Institute of Technology, Pasadena, CA, 269 (1995); J. Kawamura, R. Blundell, C.-Y.E. Tong, G. Gol'tsman, E. Gershenzon, B. Voronov, Proc. of 6th Intl. Symp on Space THz Technology, California Institute of Technology, Pasadena, CA, 254, (1995)).

TABLES

TABLE I. Device parameters and mixer results

Device	L[a] (μm)	R_N (Ω)	Opt. V_{dc}/I_{dc} (Ω)	gain dV/dI (Ω)	$T_{out,fl}(0)$[b] (K)	f_{3dB} (GHz)	Over V_{dc}/I_{dc} (Ω)	pumped dV/dI (Ω)	$T_{out,fl}(0)$ (K)	f_{3dB} (GHz)
A	0.08	54	25	57	49	6.1	38	40	7	>> 6
B	0.16	77	42	72	30	2.0	31	94	7	>> 3
C[c]	0.24	96	-	-	-	-	-	-	-	-
D	0.6	93	32	500	78	0.79	26	100	222	0.4
E	3	98	16	250	139	0.33	33	84	87	0.36

[a] $\pm$ 0.05 μm

[b] This is the low frequency contribution of the thermal fluctuation noise to the output noise.

[c] The spectrum of the noise was not measured for device C.

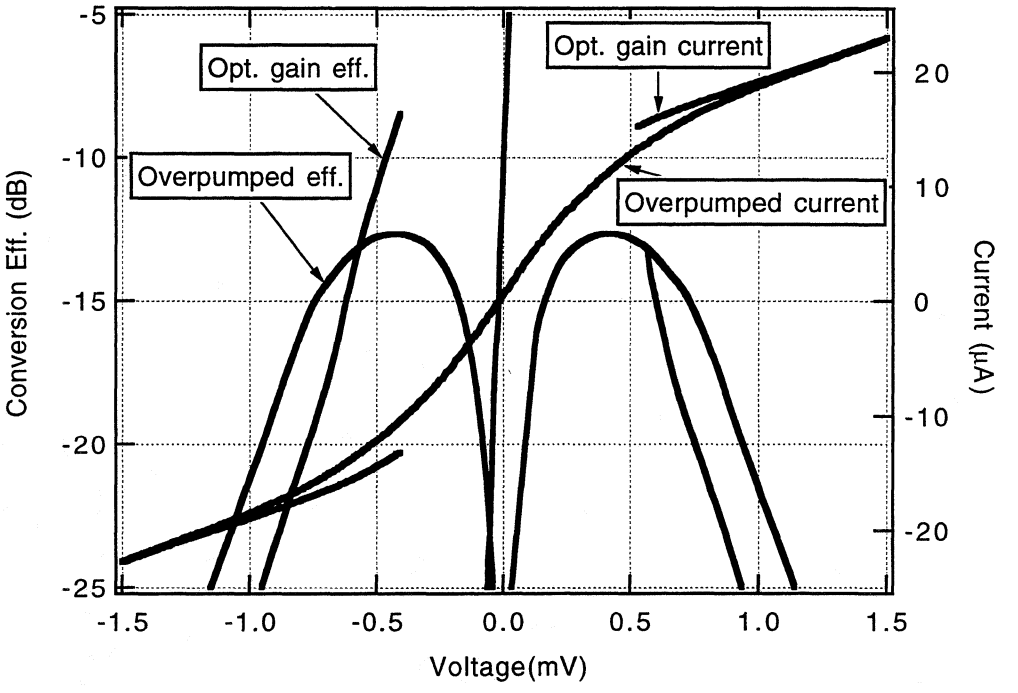

A

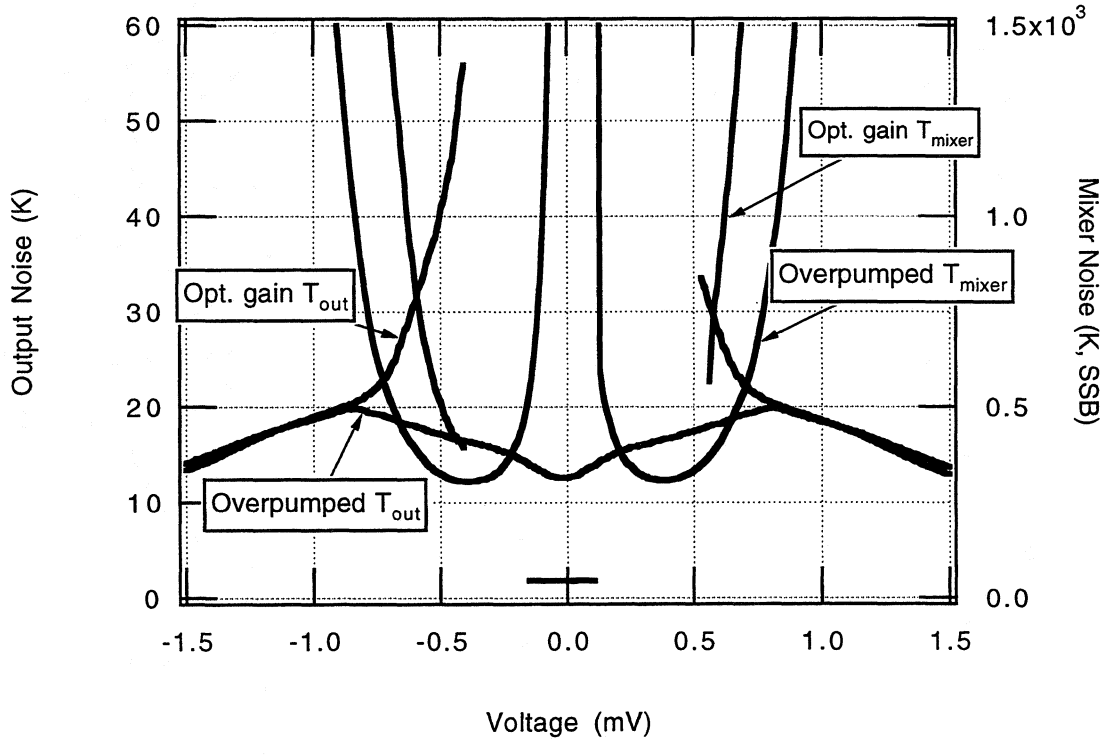

B

Figure 1: Mixer noise vs. voltage, dev. C, L=0.24 μm.
Both positive and negative voltages are plotted. The slight asymmetry is due to the device switching into the supercurrent in different ways depending on the direction of sweep.

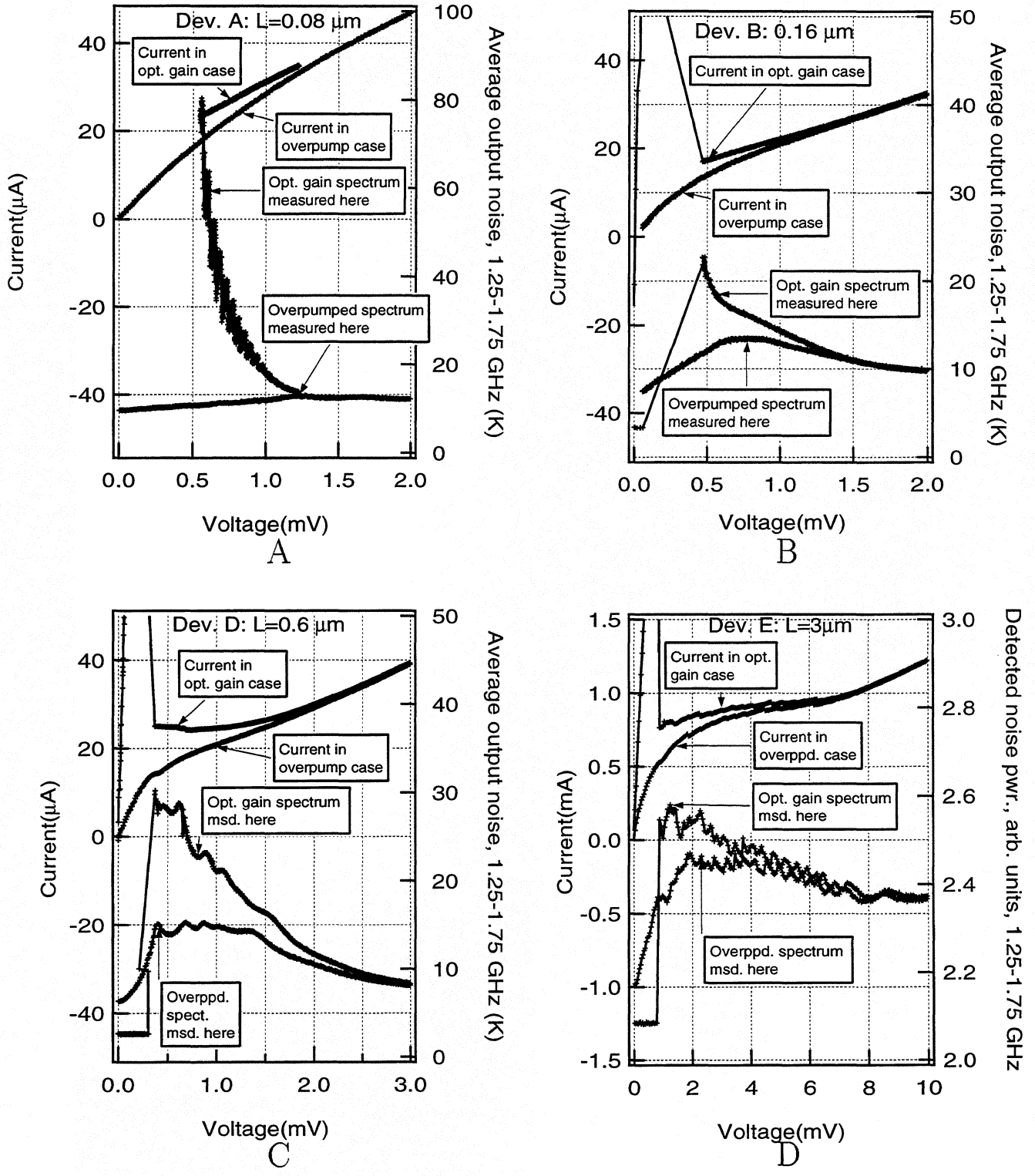

Figure 2: Avg. output noise, 1.25-1.75 GHz and current vs. voltage. Only positive bias voltages are shown; the noise and current are symmetric. In A, the supercurrent branch is not shown. In B-D, the line connecting the supercurrent branch to the resistive branch merely indicates the switch; that region of voltage is inaccessible. In D, the detected noise power includes the amplifier noise, and is uncalibrated.

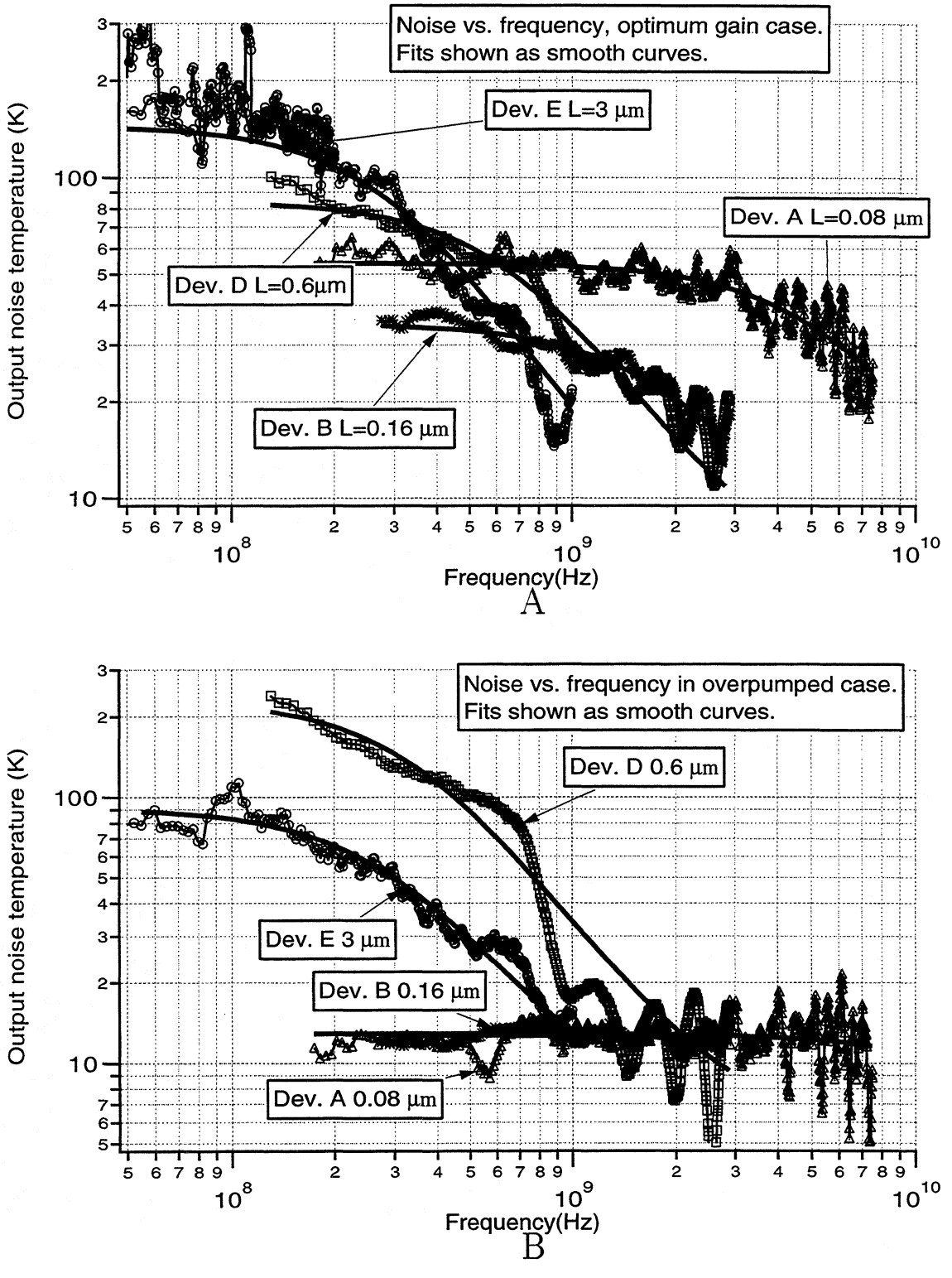

Figure 3: Output noise vs. frequency.
The smooth curves are fits to the form of Eq. (1), plus a constant term of 5.5 K due to Johnson noise. The data for the 0.6 μm device in B extend to 2.9 GHz.

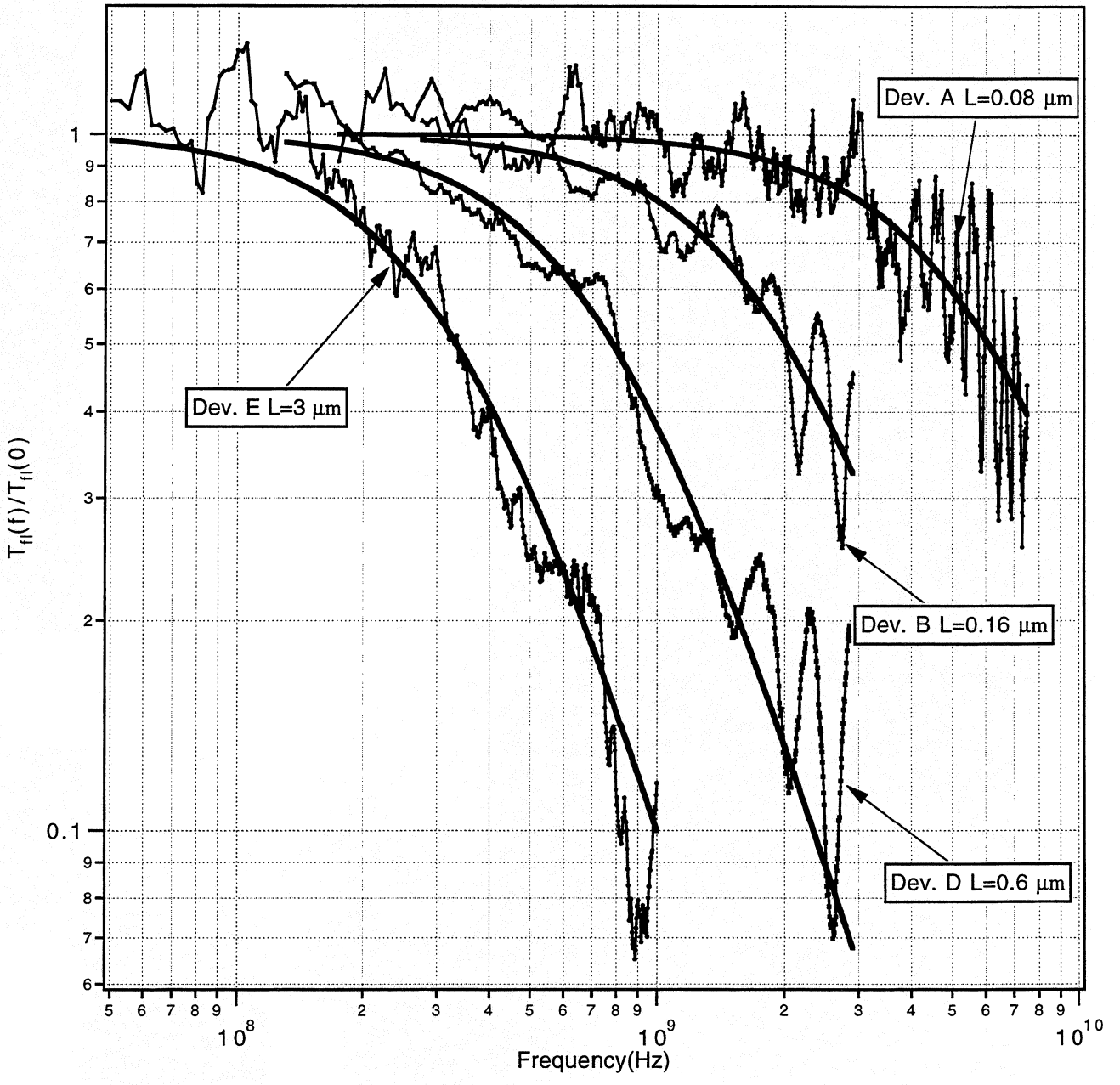

Figure 4: Relative fluctuation noise vs. frequency.
The Johnson noise of 5.5 K is subtracted off the measured output noise; the resultant noise is the thermal fluctuation noise. The fluctuation noise is plotted here, normalized to its low frequency value. The lines are the theoretical predictions, according to Eq. (1).